Sublimation origin of negative deuterium excess observed in snow and ice samples from McMurdo Dry Valleys and Allan Hills Blue Ice Areas, East Antarctica

Jun Hu[1*], Yuzhen Yan[1*], Laurence Y. Yeung[1,2], and Sylvia G. Dee[1]

[1]Department of Earth, Environmental & Planetary Sciences, Rice University, Houston TX 77005, USA.

[2]Department of Chemistry, Rice University, Houston TX 77005, USA.

Corresponding authors: Jun Hu (jun.hu@rice.edu) and Yuzhen Yan (yuzhen.yan@rice.edu)

[*]These authors contributed equally to this work.

Key Points:

- Negative deuterium excess values exist in surface snow in the McMurdo Dry Valleys and Allan Hills Blue Ice Area, East Antarctica.
- To yield negative deuterium excess in Antarctic precipitation, unrealistic moisture contribution from high-latitude oceans is required.
- Sublimation fractionation contributes to negative deuterium excess in relatively dry, windy, and relatively warm conditions.

Abstract

The oxygen and hydrogen isotopic composition in snow and ice have long been utilized to reconstruct past temperatures of polar regions, under the assumption that post-depositional processes such as sublimation do not fractionate snow. In low-accumulation (< 0.01 m yr^{-1}) areas near the McMurdo Dry Valleys in Antarctica surface snow and ice samples have negative deuterium excess values ($\delta D - 8*\delta^{18}O$). This unique phenomenon, only observed near the Dry Valleys, is not fully understood. Here we use both an isotope-enabled general circulation model and an ice physics model and establish that negative deuterium excess values can only arise from precipitation if the majority of the moisture is sourced from the Southern Ocean. However, the model results show that moisture sourced from oceans north of 55° S contributes significantly (>50%) to precipitation in Antarctica today. We thus propose that sublimation must have occurred to yield the negative deuterium excess values in snow observed in and near the Dry Valleys and that solid-phase-diffusion in ice grains is sufficiently fast to allow Rayleigh-like isotopic fractionation in similar environments. We calculate that under present-day conditions at the Allan Hills outside the Dry Valleys, 3 to 24% of the surface snow is lost due to sublimation. Because a higher fraction of snow is expected to be sublimed when accumulation rates are lower, the magnitude of $\delta^{18}O$ and δD enrichment due to sublimation will be higher during past cold periods than at present, altering the relationship between the snow isotopic composition and polar temperatures.

Plain Language Summary

Earth's past temperatures in the polar regions are often calculated from the relative abundance of heavy hydrogen or oxygen atoms (isotopes) in the polar ice. It is often assumed that, once the snow has fallen from the sky and reached the surface of the ice sheet, its isotopic composition no

longer changes. Yet, this conventional notion is incompatible with some observations. In and near the McMurdo Dry Valleys in Antarctica, for example, a unique glaciological phenomenon is that the d-excess values, defined as the relative abundance of heavy hydrogen atoms to the abundance of heavy oxygen atoms times a factor of 8, are negative. Negative d-excess values are rare in precipitation and therefore hint at the role of sublimation in causing the ice to change its isotopic composition (to "fractionate"), challenging the conventional wisdom. Here, we investigate whether the negative d-excess could originate from Antarctic precipitation and determine that it is unlikely given where the moisture arriving at Antarctica today is coming from. Therefore, we conclude that sublimation does fractionate isotopes in and near the Dry Valleys, and may affect the past temperatures reconstructed from the hydrogen and/or oxygen isotopes.

1. Introduction

1.1. Isotope paleothermometry in polar ice

The stable isotopes of oxygen and hydrogen in polar ice caps have been widely used to infer the past temperature of the polar regions (Grootes et al., 1993; J. Jouzel et al., 2007; Petit et al., 1999). This approach was initially developed from the positive correlation between the isotopic composition of precipitation and mean annual surface air temperatures (Dansgaard, 1964; Lorius et al., 1969) and was subsequently refined using alternative thermometers [e.g., borehole temperatures and etc. (Cuffey & Clow, 1997)] and, most recently, isotope-enabled atmospheric general circulation models (Holloway et al., 2018). In Antarctica today, the relationship between the surface snow $\delta^{18}O$ value (a measure of its $^{18}O/^{16}O$ ratio; the δ notation here is defined as $R_{Sample}/R_{Standard}$ - 1, in which R is the isotopic ratio of interest) and mean annual

surface air temperature has a slope of 0.8‰/°C. This slope is derived from measurements performed at many different sites in Antarctica, and hence is referred to as the "spatial" $\delta^{18}O$ slope (Masson-Delmotte et al., 2008). It can be qualitatively explained as the result of Rayleigh-style fractionation during vapor condensation, with the condensation temperature being the most important parameter. This simple yet informative framework yields the longest Antarctic temperature record, a continuous 800-thousand-year (kyr) time-series, from the D/H ratios (expressed as δD) in the EPICA Dome C (EDC) ice core drilled in East Antarctica (J. Jouzel et al., 2007).

However, where independently-reconstructed temperature is available, the isotope-temperature sensitivity recorded in a single ice core over time (i.e., a "temporal" slope) has been shown to deviate from the spatial slope (Cuffey et al., 2016; Cuffey & Clow, 1997). For example, at Taylor Dome, situated near the McMurdo Dry Valleys, East Antarctica, an ice core isotope record shows a temporal $\delta^{18}O$ slope of 0.5‰/°C (Steig et al., 2000). Similarly, in Greenland, where the modern-day spatial $\delta^{18}O$ slope is 0.7‰/°C (Dansgaard, 1964), the temporal slope varied between 0.2‰/°C and 0.6‰/°C from the Last Glacial Maximum into the early Holocene (Buizert et al., 2014). Applying the conventional 0.8‰/°C spatial slope to isotope records obtained from those sites would underestimate the temperature difference, especially that associated with glacial cooling. In any case, processes in addition to condensation and precipitation over Antarctica must alter the isotope-temperature relationship recorded in ice cores.

To shed light on these additional processes, deuterium excess (d-excess), a second-order parameter defined as $\delta D - 8 \times \delta^{18}O$, is often utilized (Dansgaard, 1964). Deuterium excess in meteoric water is affected by several physical processes central to the global hydrological cycle

(Figure 1). Importantly, d-excess is insensitive to isotope fractionation at equilibrium, such as the transition from vapor to liquid, but sensitive to kinetic fractionation (Dansgaard, 1964). Observations show that the d-excess of water vapor above the ocean surface has a typical range of ~+30‰ to ~0‰, and exhibits a negative correlation with relative humidity (RH) and a positive correlation with sea surface temperature (SST) (Benetti et al., 2014; Gat et al., 2011; Ryu Uemura et al., 2008). This relationship between vapor d-excess, RH and SST is believed to result primarily from evaporation, which is rate-limited by diffusive transport across the boundary layer separating the liquid and the free atmosphere. In one oft-used evaporation model (Craig & Gordon, 1965), water vapor immediately above the evaporating liquid is in phase and isotopic equilibrium with the liquid below, resulting in a δD vs. $\delta^{18}O$ slope of ~8 and little to no change in d-excess values. Vapor transport into the free atmosphere is largely diffusion-controlled, leading to diffusive isotopic fractionation: HDO diffuses roughly twice as fast as $H_2{}^{18}O$ (compared to $H_2{}^{16}O$), causing isotopic fractionation along a slope of ~0.5 and a deuterium excess in the vapor. The humidity gradient between the free atmosphere (RH < 1) and the fully saturated interface (RH = 1) modulates the magnitude of this fractionation. Evaporation at low SST and high RH leads to a weak diffusive fractionation and results in low vapor d-excess that might produce precipitation with negative d-excess.

An additional process leading to kinetic fractionation is the phase change between water vapor, supercooled liquid, and solid ice in clouds during snow formation (Yau & Rogers, 1996). The water vapor pressure inside clouds is higher than the saturation vapor pressure over ice, but lower than the saturation vapor pressure over liquid water (Jean Jouzel & Merlivat, 1984). The liquid-to-solid transition will therefore take place in two steps, first through evaporation and then condensation. Both processes involve kinetic isotope fractionation as the phases are not in

113 equilibrium (Ciais & Jouzel, 1994). The three-phase interaction will persist until the ambient
114 temperature drops below the deliquescence point where supercooled liquid no longer exists.
115 After that, supersaturation of vapor over the solid will dominate the kinetic fractionation.

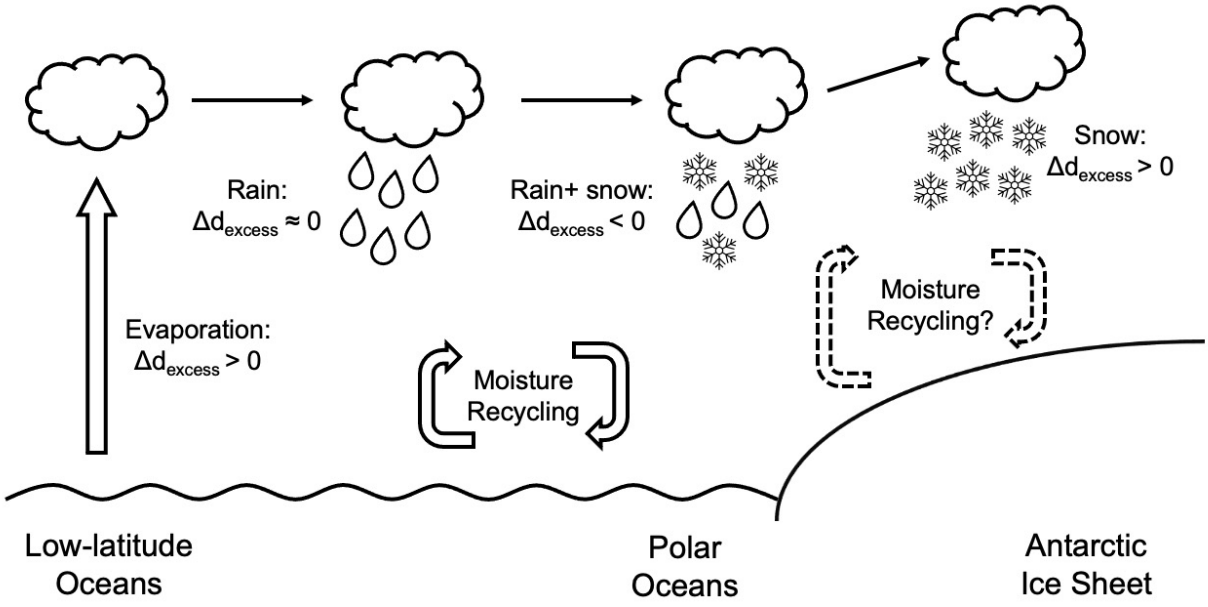

116

117 **Figure 1.** Schematics of the hydrological and post-depositional processes relevant to Antarctic
118 precipitation and their respective impact on d-excess. Δd_{excess} is defined as the d_{excess} of the
119 product (e.g. vapor) minus the d_{excess} of the reactant (e.g. ocean).

120

121 Last, applications of the water/ice isotopic paleothermometer often assume that $\delta^{18}O$, δD,
122 and d-excess values do not change due to post-depositional processes, such as snow
123 metamorphism and sublimation after precipitation has occurred. In studies where post-
124 depositional modifications to isotope records have been explicitly considered, the focus has
125 largely been the attenuation of seasonal to annual climate signals due to diffusive smoothing,
126 with an ultimate goal of retrieving the original high-frequency signals (Hughes et al., 2020; Jones

et al., 2017; Whillans & Grootes, 1985). On timescales where diffusive smoothing is not important, the stable water isotope records are often interpreted without accounting for the effect of sublimation, a process that has been subject to increasing scrutiny.

1.2. Does sublimation cause isotopic fractionation in snow?

The prevailing view that sublimation does not cause isotopic fractionation arises from two key assumptions:

A. Sublimation of snow and ice occurs "layer-by-layer" (Friedman et al., 1991).

B. The sublimed vapor is immediately "removed" from the ice surface and no re-condensation occurs.

However, this view is incompatible with many field observations. (Moser & Stichler, 1974) first reported the enrichment of surface snow δD by 25‰ associated with net mass loss in snow samples collected in the Swiss Alps over the course of a week. Increases in surface firn $\delta^{18}O$ values concurrent with sublimation was also observed in high-altitude glaciers in the tropical Andes (Stichler et al., 2001). These observations made on ice at high elevations clearly demonstrate mass flux and isotopic exchange between snow and water vapor in the atmosphere (Moser & Stichler, 1974).

Yet in much colder environments such as Antarctica, isotopic fractionation due to sublimation has been largely omitted for two reasons. First, vapor saturation pressure scales with temperature following Clausius–Clapeyron equation, and thus the low vapor content in polar environments is not often considered capable of modifying the isotopic composition of the firn (Waddington et al., 2002). Second, the rate of sublimation is also lower at colder temperatures, and the impact (if any) is considered to be limited to the top of the ice layer (Jean Jouzel et al.,

1982). Therefore, ice-core δD and $\delta^{18}O$ records are often used for paleotemperature reconstructions without correcting for sublimation-induced fractionation (Petit et al., 1999). Lately, however, a growing number of field observations has revealed significant mass exchange between surface snow and atmospheric water vapor through daily sublimation-condensation cycles (Casado et al., 2018; Li et al., 2021; Madsen et al., 2019; Ritter et al., 2016; Steen-Larsen et al., 2014). As a result, Assumption (B), that no vapor re-condenses on surface snow, appears to be invalid. The extent of post-depositional modification to the observed ice-core δD and $\delta^{18}O$ time-series remains unclear, however, because the δD and $\delta^{18}O$ values of past vapor are not known.

More fundamental, perhaps, is whether the "layer-by-layer" model of sublimation is valid over the entire range of Antarctic environments (Assumption A). Does surface snow remain unfractionated at sites with extremely low accumulation rate, strong surface wind, low atmospheric vapor content, and largely unidirectional vapor flux (from snow into the atmosphere)? In modern-day Antarctica, such conditions are found in and near Blue Ice Areas (BIAs), where crystalline ice previously buried in ice sheets is now exhumed at the surface (Bintanja, 1999; Bliss et al., 2011; Spaulding et al., 2012). Even in accumulation zones adjacent to the BIAs, conditions conducive to sublimation after snow has been deposited still exist, providing an opportunity to investigate whether ice sublimation causes isotopic fractionation in the field (Dadic et al., 2015). Again, deuterium excess can serve as a useful diagnostic tool. If sublimation, a non-equilibrium process, does cause isotopic fractionation in ice, d-excess should be affected in a manner similar to evaporation: the d-excess of the sublimed vapor increases while the remaining snow d-excess decreases. Laboratory studies on sublimation of snow and ice

samples under RH < 1 and isothermal conditions indeed show a lowering of d-excess as sublimation progresses over 60 days (Sokratov & Golubev, 2009).

Intriguingly, while most of the d-excess values observed in present-day Antarctic surface snow are positive (Masson-Delmotte et al., 2008), a notable exception can be found in the McMurdo Dry Valleys and the nearby (~100 km away) Allan Hills Blue BIAs where conditions are persistently dry and windy: surface snow samples consistently show negative d-excess values (Dadic et al., 2015; Gooseff et al., 2006; Masson-Delmotte et al., 2008). Two physical mechanisms can explain this observation of negative d-excess values:

A. Water vapor originates from a high-latitude, local moisture source, where high RH and low SST yields an equilibrium δD vs. $\delta^{18}O$ slope slightly higher than 8 (Gooseff et al., 2006; Higgins et al., 2015).

B. Sublimation causes isotopic fractionation in snow (Dadic et al., 2015; Gooseff et al., 2006; Masson-Delmotte et al., 2008).

No investigation has been conducted to evaluate the role of these two mechanisms in generating the negative d-excess observed in the Dry Valleys and the Allan Hills, which we aim to examine in the present study. We first perform a water-tagging experiment using the isotope-enabled general circulation model iCESM (J. Nusbaumer et al., 2017) to determine the climatological factors controlling the deuterium excess of precipitation over the Dry Valleys region. We then evaluate the potential importance of precipitation-sourced negative d-excess values compared to that from sublimation fractionation. What physical mechanisms allow sublimation to fractionate isotopes in the ice and snow is also discussed.

Post-depositional changes to isotopic composition of surface snow near the Dry Valleys have implications for temperature reconstructions based on the δD and $\delta^{18}O$ records in Allan Hills blue ice, where the oldest ice samples are as old as 2.7 million years (Yan et al., 2019). More importantly, because the very low accumulation rates recorded in Allan Hills have often been seen as a modern analogue to past glacial conditions (Dadic et al., 2015), sublimation may become an important factor in altering the isotopic composition of water at other sites during glacial intervals, when the degree of sublimation is different from present-day conditions. We close with a discussion of the implications of post-depositional sublimation for temperature reconstruction from ice cores drilled in and near the Dry Valleys, and suggest updates to isotope-enabled climate model physics, which currently treat post-depositional sublimation of ice and snow as non-fractionating (Dütsch et al., 2019).

2. Methods

2.1 Isotope-Enabled General Circulation Model Experiments

A stable water isotope-enabled climate model, the isotope-enabled Community Earth System Model (iCESM) (Brady et al., 2019; J. Nusbaumer et al., 2017), was employed to examine the factors controlling the snowfall d-excess values at Allan Hills. iCESM simulates known isotopic fractionation processes, including equilibrium fraction during the condensation of water vapor, kinetic fractionation during evaporation from the oceans, rainfall evaporation, and ice deposition in clouds. Importantly, the model can conduct moisture-tagging experiments: within a given simulation, one can track the isotopic composition of a parcel of air once moisture evaporates from the surface in a specific ocean or land region. This water-tagging technique has been used to track moisture and the isotopic composition of water in several earlier studies (Bailey et al., 2019; Dyer et al., 2017; Hu et al., 2019; Jesse Nusbaumer & Noone, 2018; Singh

et al., 2016; Tabor et al., 2018; Wang et al., 2020). The tag follows the life cycle of moisture through all advection and condensation processes until that moisture leaves the atmosphere as precipitation.

To study the seasonal and interannual variability of modern-day snowfall d-excess at Allan Hills, we conducted an experiment using prescribed sea-surface temperature and sea-ice observations from 1977–2012. While the focus of the present study is modern-day climatological d-excess, similar simulations could also shed light on past d-excess variations if different (e.g. glacial) boundary conditions were used. The water vapor is tagged according to its origin from among the 25 regions shown in Figure S1. The resolution of the atmospheric model is 1.875° × 2.5° (latitude × longitude) with 30 vertical layers.

The mass ratios of precipitation $H_2{}^{18}O/H_2O$ and HDO/H_2O at each grid cell are computed as the sum of the ratios originating from all tagged regions, weighted by their precipitation contribution:

$$R_P = \sum_{i=1}^{25} R_{Psinki} \times \frac{P_i}{P_{total}} \quad (1)$$

where *i* indexes a tagged region, and R_{Psinki} and P_i are the isotopic ratios and precipitation fluxes falling in the given grid cell (i.e., the "sink"), derived from water vapor originating from the *i*th tagged region. P_{total} is the total precipitation at this grid cell. We then calculate precipitation $\delta^{18}O$, δD, and d-excess values relative to Vienna Standard Mean Ocean Water (VSMOW) by using the isotopic ratios R_P.

iCESM simulates precipitation, the isotopic composition of precipitation, and their seasonal cycles in polar regions reasonably well (Wang et al., 2020). However, we caution that there is a known bias in absolute precipitation $\delta^{18}O$ and d-excess values (Brady et al., 2019). We

therefore evaluated the model output with ice core d-excess observations at five sites: South Pole, Dome F, West Antarctic Ice Sheet (WAIS) Divide, Talos Dome, and Taylor Dome. We did not include other well-known East Antarctic sites such as Vostok and Dome C, because the temporal resolution of the stable water isotope records from those sites is too low to allow meaningful comparison. Of particular importance is the model-data comparison in Taylor Dome, because the McMurdo Dry Valleys and Allan Hills are nearby (within ~100 km). We can thus use the Taylor Dome model-data comparison to calibrate the Dry Valleys and Allan Hills precipitation d-excess simulated by iCESM.

2.2 Mixed-Cloud Isotope Model

As a complement to the iCESM fully coupled model experiments, we used a Mixed-Cloud Isotope Model (MCIM) and explored the range of precipitation d-excess values from a single source with given SST and RH. The MCIM calculates the fractionation of water isotopes as a function of decreasing temperature in clouds, in which the coexistence of vapor, liquid, and ice causes kinetic fractionation (Ciais & Jouzel, 1994). Two non-equilibrium processes are of particular importance: the transition of liquid droplets into water vapor and the condensation of supersaturated vapor onto ice crystals. The underlying physical mechanisms are also included in the atmospheric module of iCESM (Brady et al., 2019; Dütsch et al., 2019). The MCIM model has been widely implemented to simulate and help interpret the isotopic composition of precipitation in polar regions (Casado et al., 2016; Pang et al., 2019; Vimeux et al., 1999).

In the MCIM, the isotopic composition of vapor, cloud, and precipitation are calculated from three sets of input variables: (1) the initial conditions (SST and RH) at the moisture source region, (2) the supersaturation parameter (S) during snow formation, and (3) the temperature at which condensation and precipitation occurs (Ciais & Jouzel, 1994). Because SST and RH is

prescribed according to observations and precipitation temperature is the independent variable, the supersaturation parameter (S) is the most important parameter in determining the accurate isotopic composition of precipitation with the following mathematical formulation:

$$S = p + q*T \quad (2)$$

T is the condensation temperature (in degree Celsius), and p and q are two tunable parameters (Ciais & Jouzel, 1994). This set of variables are calibrated against observed spatial distribution of d-excess in modern East Antarctic surface snow (Jean Jouzel & Merlivat, 1984; Petit et al., 1991). For precipitation at a single site, slope p and intercept q values should ideally be calibrated against a time-series of precipitation d-excess and δD at that specific site (Pang et al., 2019). However, due to a lack of continuous observations of precipitation d-excess near Allan Hills BIAs and the Dry Valleys, it is not possible yet to calibrate p and q. We therefore tested the sensitivity of precipitation d-excess to different choices of q (-0.002 to -0.006) while assuming a fixed p value of 1, following the treatment of (Dütsch et al., 2019). The assumption of an invariable p is justified by its physical constraint, which is that supersaturation starts to occur at $T = 0$ °C, where p should be close to 1. We then asked under what circumstances negative d-excess values can exist in Antarctic precipitation.

3. Results

3.1 Model Isotope Climatology

We first evaluated the climatology of d-excess values in precipitation over the entirety of Antarctica, calculated as the 36-year-average yearly d-excess values in Antarctic precipitation between 1977 and 2012 (Figure 2a). Also shown are monthly mean values for January (Figure 2b) and July (Figure 2c), representing austral summer and winter, respectively, to demonstrate

the intra-annual variability of precipitation d-excess values. Spatially, the model result shows d-excess values over West Antarctica are generally 10-15‰ lower than d-excess values in East Antarctica. This contrast likely exists because a higher fraction of West Antarctic precipitation is sourced from the Southern Ocean, where water vapor d-excess values are lower. In contrast, East Antarctica receives more moisture sourced from lower latitudes, where water vapor d-excess values are higher (Bailey et al., 2019). Within East Antarctica, precipitation over coastal regions has lower d-excess values than those from the East Antarctic Plateau. The spatial pattern of d-excess reconstructed in the model is consistent with surface d-excess observations [Figure 3 in (Masson-Delmotte et al., 2008)].

When compared to observational data, the absolute d-excess values simulated by the model are 1.6 to 8.9‰ lower than the observations in nearly all of West Antarctica and most of the coastal regions in East Antarctica (Table 1 and Figure 2a). We note that this negative bias in d-excess is also found in other iCESM simulations, possibly linked to an overestimation of ice crystal growth rate in clouds (Dütsch et al., 2019). Despite the offset in mean d-excess values, a comparable temporal d-excess variability, represented by the standard deviation of yearly d-excess values, is found between the model output and the ice core (South Pole, Dome Fuji, WAIS, Taylor Dome, and Talos Dome) data (Table 1). We therefore argue that the model is still useful in quantifying the contributions of different moisture sources and the associated large-scale circulation to precipitation d-excess. Importantly, the observed model-data difference (model minus data) of d-excess in Taylor Dome, which the Allan Hills and Dry Valleys are located next to, is -6‰. A model-data offset of similar magnitude (-5‰) is also found in Talos Dome (72°48’S, 159°06’E; ~500 km from the Allan Hills/Dry Valleys) in our model output.

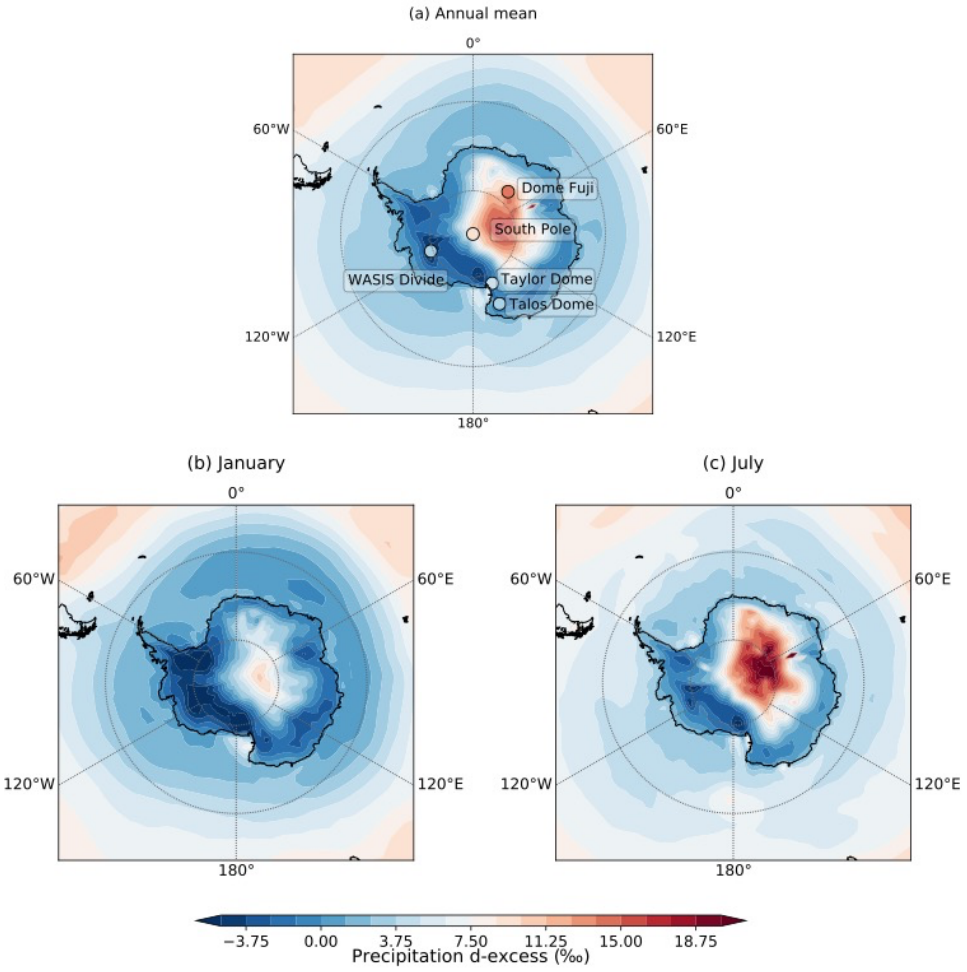

304

305 **Figure 2.** (a) Climatological precipitation d-excess simulated by iCESM (1977-2012 CE) and ice
306 core measurements (post 1840 CE). (b) Climatological precipitation d-excess simulated by
307 iCESM (1977-2012 CE) in January over Antarctica. (c) Same model output as in (b) but for the
308 month of July.

309

310 Applying a simple +6‰ correction to the d-excess values of modeled Allan Hills
311 snowfall thus yields mean surface snow d-excess values of 3.9 ± 0.7‰ (1σ) and 4.8 ± 0.7‰ in
312 the Dry Valleys and Allan Hills, respectively. The model output is on average 6.7‰ higher than
313 the observed snow d-excess values in the Dry Valleys and Allan Hills, which are -1.8 ± 5.9‰

(Gooseff et al., 2006) and -2.9 ± 2.8‰ (Dadic et al., 2015), respectively. We note that the iCESM output shows less d-excess variability than do the actual observations in both Dry Valleys and Allan Hills. In the case of the Dry Valleys, such a discrepancy could arise from the fact that observations were made on fresh surface snow collected in the year 1996 and thus represent the spatial, instead of temporal, d-excess variability (Gooseff et al., 2006). In Allan Hills, the larger variability in the observed data might arise from model grid resolution and/or elevation, or be caused by processes that are not captured by the model, such as post-depositional modifications.

Table 1. Comparison of iCESM-simulated climatological precipitation d-excess between 1977 and 2012 CE against ice core or surface snow d-excess measurements. Errors represent one standard deviation of d-excess values.

Location name (Lon., Lat.)	**iCESM result**	**Observations**	**Observation Interval**	**Sampling Resolution**	**Refs.**
South Pole (-98.16°, -89.99°)	8.2 ± 1.3‰	9.8 ± 0.9‰	1977-2012	1 year[a]	(Steig et al., 2021)
WAIS Divide (-112.09°, -79.47°)	-5.4 ± 0.5‰	3.5 ± 1.0‰	1842-2004	~3 years	(Jones et al., 2018)
Dome Fuji (39.70°, -77.32°)	10.5 ± 1.7‰	14.1 ± 1.3‰	1860-1970	~20 years	(R. Uemura et al., 2012)
Talos Dome (159.18°, -72.82°)	-1.6 ± 0.6‰	3.5 ± 1.2‰	1846-1991	~6 years	(Mezgec et al., 2017)

Taylor Dome (158.00°, -77.67°)	-1.2 ± 0.8‰	4.8 ± 0.8‰	1846-1955	~8 years	(Vimeux, Masson, Jouzel, et al., 2001)
McMurdo Dry Valleys (162.78°, -77.64°)	-2.1 ± 0.7‰	-1.8 ± 5.9‰	1996[b]	N/A	(Gooseff et al., 2006)
Allan Hills Blue Ice Area (159.23°, -76.67°)	-1.2 ± 0.7‰	-2.9 ± 2.8‰	1991-2011[c]	~1 year	(Dadic et al., 2015)

[a] Raw South Pole ice core stable water isotope data were measured at sub-annual timescales. We pre-averaged the high-resolution data to obtain the yearly means in order to calculate the climatological mean and the standard deviation. Not all other ice core data have such a high temporal resolution.

[b] Samples from the McMurdo Dry Valleys are all surface fresh snow. We thus assumed a constant age. The standard deviation in snow d-excess reflects the spatial heterogeneity, and we caution against comparing the modeled temporal variability with the observed spatial variability.

[c] Allan Hills observation interval corresponds to the top 30 cm in a 5-m firn core. The age of that 30-cm top section (20 years) was determined by a single ^{210}Pb-activity measurement (Dadic et al., 2015). Since no age constraint was available below this depth, we only included the data from the top 30 cm.

3.2 Controls on d-excess in Allan Hills precipitation: water tagging experiments

To explore the controls on d-excess values of precipitation over Allan Hills and Dry Valleys, we next conducted iCESM water tagging experiments. Following the framework introduced in (Tabor et al., 2018), the change in precipitation d-excess can be decomposed into four parts: (1) the fractionation due to evaporation at moisture sources (Δd_wv_source); (2) the

fractionation along the moisture trajectory, which is the difference between the water vapor d excess value at Allan Hills and that at moisture sources (Δ(d_wv_AH-d_wv_source)); (3) the fractionation due to condensation/deposition processes at Allan Hills (Δ(d_snow_AH-d_wv_AH)); and (4) the change in d-excess value due to the change in moisture source contribution from each tagged region ($\Delta(P_i/P_{total})$, cf. eq. 2). We then calculated the composite difference between negative and positive d-excess anomaly years. A positive or negative anomaly is defined when snowfall-weighted annual mean d-excess is one standard deviation above or below the long-term mean d excess, respectively (Figure 3). At Allan Hills, the difference between the negative and positive anomaly of snowfall d-excess is about -1.3‰.

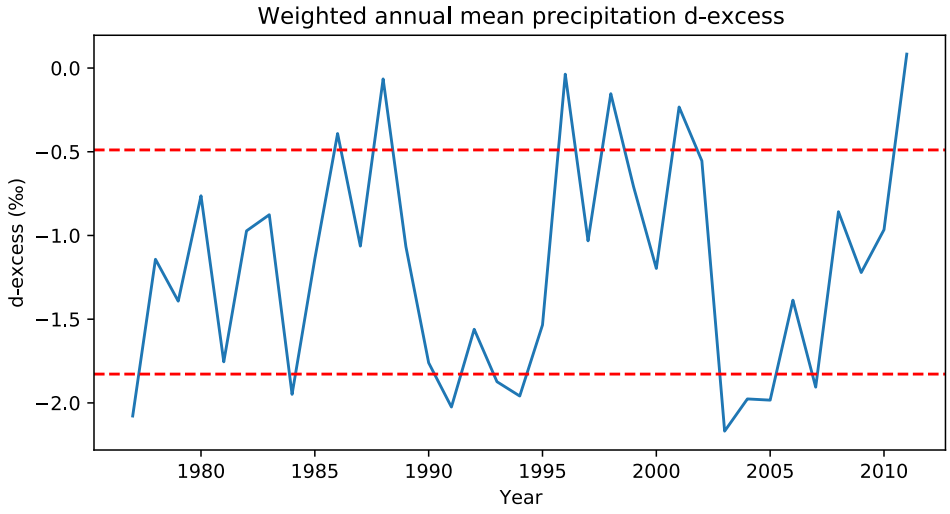

Figure 3. Interannual variability of d-excess at Allan Hills precipitation simulated by iCESM. Red dashed lines mark the one standard deviation above or below the long-term mean d excess.

Using the framework above, we find that the moisture source changes (the 4th part of the d-excess change) are the largest contributing factor to precipitation d-excess variability (Figure 4 and Table 2). Moisture originating from the Ross Sea and Amundsen Sea has lower d-excess

values than vapor from more distant oceans due to the higher RH and lower SST at these two high-latitude polar oceans (Figure S2). Previous observational studies (Benetti et al., 2014; Pfahl & Sodemann, 2014) have shown that low water vapor d-excess at the marine boundary layer is associated with high relative humidity and low SST. A 0.83‰ decrease (64% of the total change) in Allan Hills precipitation d-excess during negative-anomaly years can be attributed to an increased contribution of Ross- and Amundsen-Sea moisture (Table 2). An overestimation of moisture contribution from the high-latitude oceans in Allan Hills precipitation (due to the coarse model resolution employed in this study) may also help explain why iCESM underestimates the climatological d-excess in Allan Hills precipitation. The altitude of Allan Hills is around 1500 m, but in the model, the average topography of Allan Hills is approximately 1000 m. The lower altitude of the study site in the model leads to excess moisture sourced from the nearby ocean regions, bringing water vapor with more negative d-excess values.

A secondary effect associated with changes to the moisture trajectory accounts for a 0.37‰ change in snowfall d-excess, corresponding to 29% of the total change (Figure 4 and Table 2). This effect for each ocean region is different, however, likely due to the differential changes of moisture trajectory length experienced (Figure S3). During the negative-anomaly years, moisture originating from the Ross Sea and Southern Indian Ocean has a shorter travel distance, which leads to negative precipitation d-excess anomalies; by contrast, the Southeastern Pacific Ocean contributes positive d-excess anomalies and has a longer travel distance to reach the Allan Hills. Finally, in the simulations, the contributions from water vapor composition at the moisture sources and condensation/deposition fractionation are negligible.

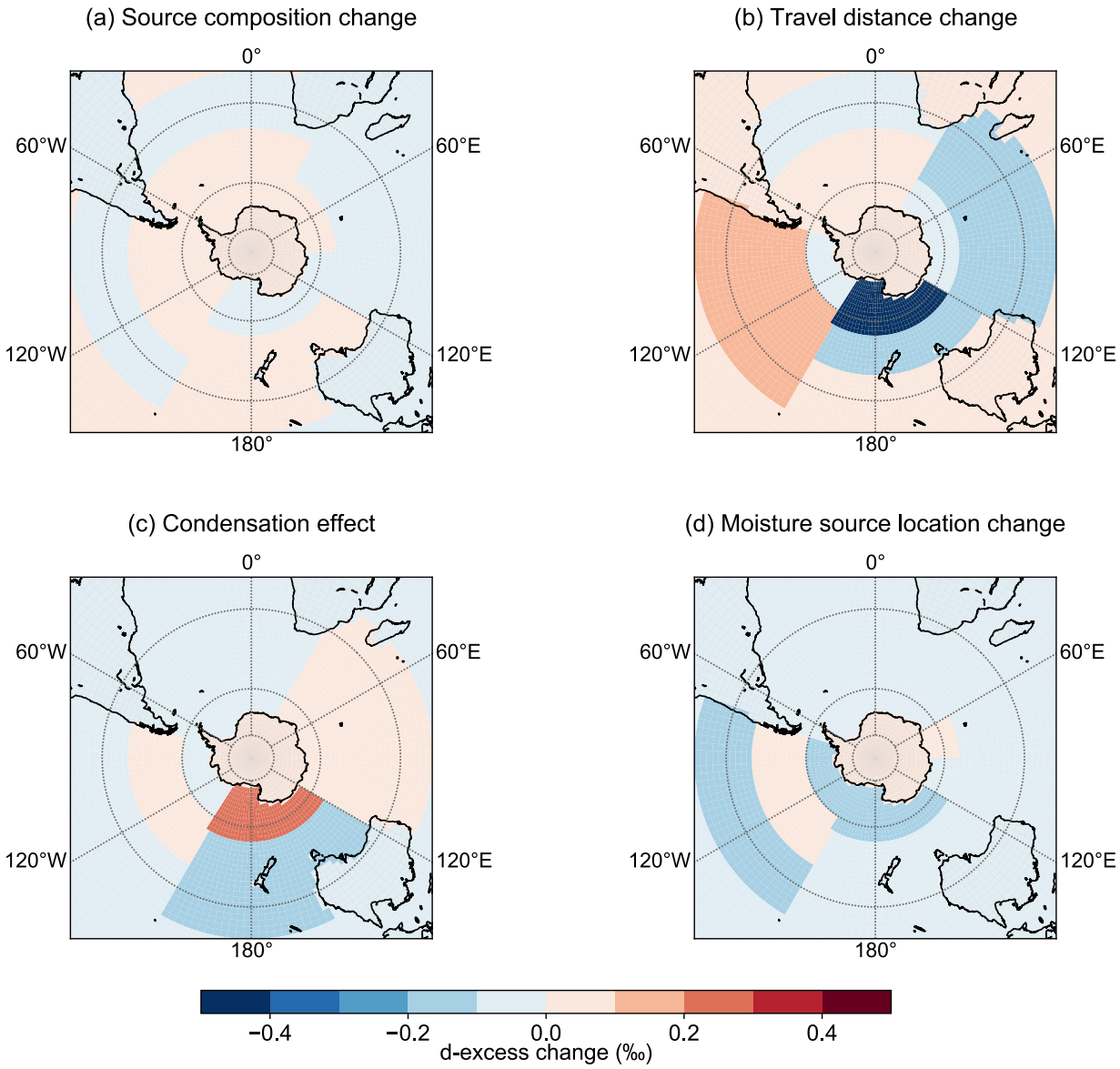

Figure 4. Quantification of the effect of source water vapor composition, fractionation along trajectory, condensation/deposition processes, and moisture source location on the difference between negative and positive d-excess anomalies (red dashed lines in Figure 3) of Allan Hills precipitation (unit: ‰).

384 **Table 2.** Quantification of different factors contributing to negative d-excess anomaly on
385 interannual timescales.

Factors	Absolute contribution	Relative contribution
Vapor composition at the source	-0.01‰	1%
Travel distance/trajectory	-0.37‰	29%
Condensation changes	-0.08‰	6%
Source location change	-0.83‰	64%
Total	-1.29‰	100%

386

387 Moreover, the years with a negative d-excess anomaly are characterized by atmospheric
388 circulation anomalies (Figure S4). In particular, a cyclonic anomaly centered at Amundsen Sea
389 and an anticyclonic anomaly north of the Amundsen Sea are associated with the simulated
390 negative d-excess anomalies. The westerlies between these two cells are strengthened. These
391 circulation anomalies also effectively block the moisture transport from the more distant
392 Southern Ocean to Allan Hills, leading to a larger moisture contribution from the nearby Ross
393 and Amundsen Seas. We note that these circulation anomalies occur mainly over the South
394 Pacific, and that only the westerlies over the Pacific are strengthened.

395 *3.3 Negative d-excess in precipitation: MCIM simulation*

396 The results from iCESM (after applying an empirical correction of +6‰ to the model
397 results) suggests that precipitation over and near the Dry Valleys should have mean d-excess
398 values that are positive on decadal timescales, but it does not fundamentally preclude a negative

d-excess in precipitation. Using the MCIM model introduced in Section 2.2, we explored under what conditions negative d-excess values can be observed in precipitation. Two moisture sources to the Allan Hills were considered: the Southern Ocean and low latitude tropical oceans. To yield the lowest d-excess end-members possible, the maximum values of RH (91% for the Southern Ocean and 83% for the tropical oceans) and minimum of sea-surface temperature (6°C for the Southern Ocean and 28°C for the tropical oceans) over 1977-2012 were fed into the MCIM. These data come from the reanalysis dataset NCEP/NCAR (Kalnay et al., 1996) and Hadley Centre Sea Ice and Sea Surface Temperature data set (Rayner et al., 2003). The MCIM then calculated the isotopic composition of water in the vapor, cloud, and precipitation as a function of precipitation temperature. Here, a linear and monotonic decrease in temperature was assumed for the traverse from source to sink, with no vapor recharge from secondary moisture sources. Note that even in the case of moisture recharge, precipitation cannot have a negative d-excess value without at least one of the end-member sources having negative d-excess values in precipitation.

Results from the MCIM simulations show that moisture originating from the Southern Ocean can yield precipitation with a negative d-excess, with values lower than -10‰ when e.g., SST is less than 6°C and RH is greater than 91% (Figure 5). By contrast, moisture evaporating from the tropical oceans never produces negative d-excess in precipitation along its trajectory, a robust feature regardless of what q values were chosen between -0.002 and -0.006 for supersaturation parameterization. In both moisture-source cases, the lowest precipitation d-excess value reached along the moisture trajectory would have little seasonal variation. The MCIM results thus confirm that negative d-excess values in Allan Hills snow and ice can be derived from precipitation if the moisture is dominantly sourced from the high-latitude Southern

Ocean. However, as the iCESM simulation shows, the subpolar ocean is also an important source of moisture that forms precipitation over the Dry Valleys and Allan Hills, accounting for more than half of the precipitation that ultimately falls at these sites (Figure S5). This conclusion is also supported by previous moisture trajectory diagnostics, where Victoria Land has a mean moisture source latitude of 42 °S (Sodemann & Stohl, 2009). Therefore, we conclude that negative d-excess values in modern Allan Hills precipitation are unlikely given the substantial input from subtropical moisture sources.

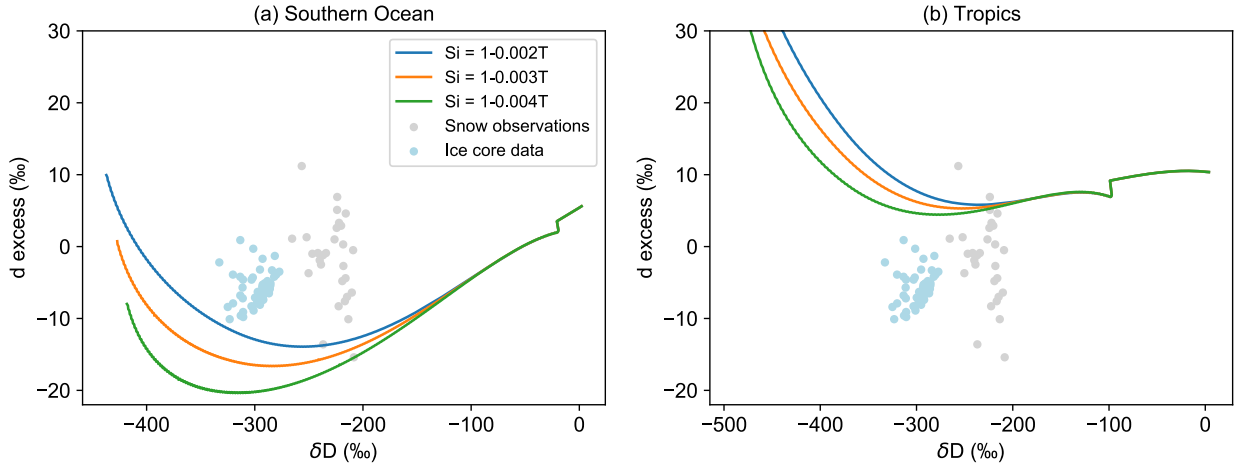

Figure 5. Modeled d-excess in precipitation along moisture trajectories if moisture solely originates from (a) the Southern Ocean and (b) the Tropical ocean for three different supersaturated parameter Si as a function of condensation temperature, with the maximum values of relative humidity and minimum values of SST from 1977 to 2012 over the regions using the Mixed-Cloud Isotope Model. Grey dots show fresh snow deuterium excess and δD values observed in the Dry Valleys (Gooseff et al., 2006). Blue dots show ice core deuterium excess and δD values observed in the Allan Hills (Higgins et al., 2015).

4. Discussion

4.1 Physical mechanisms of isotopic fractionation by sublimation

Our isotope-enabled general circulation model simulations do not support a moisture-source origin of negative d-excess values in the Dry Valleys and Allan Hills snow and ice. We therefore propose that sublimation of polar snow is not adequately described by a simple "layer-by-layer" mechanism in all cases. Instead, we suggest that solid-state diffusion and homogenization of ice grains can lead to Rayleigh-like fractionation in specific polar environments, explaining the particular occurrence and magnitude of d-excess found in the McMurdo Dry Valleys, and in particular in the Allan Hill BIAs. However, two conditions must be met for a Rayleigh-like sublimation fractionation to be recorded in ice.

First, a physical mechanism that fractionates HDO and $H_2{}^{18}O$ on a slope less than 8 must exist so the d-excess of the remaining ice can be progressively lowered. Phase equilibrium between vapor and ice at low temperature is one candidate, but its magnitude, inferred from the equilibrium fractionation factors (Ellehoj et al., 2013), is small. A stronger isotopic effect is associated with the upward diffusion of interstitial vapor into the free atmosphere that has a RH < 1. This process, however, is unlikely to be important because convective air motion dominates in the top a few meters of the firn; in some extreme cases (e.g. sites with near-zero accumulation rates and high winds), the convective layer can penetrate >20 m deep into the firn (Severinghaus et al., 2010). Most isotopic fractionation during sublimation seems to occur in the uppermost snow layers first, before propagating downwards (Moser and Stichler et al. 1974; Hughes et al. 2021) . Vapor diffusion inside the firn may therefore not be the physical mechanism responsible for the sublimation-induced isotopic fractionation investigated here, although we note that

interstitial vapor diffusion is important for dampening the high-frequency δD and $\delta^{18}O$ variability (Cuffey & Steig, 1998).

A more physically plausible mechanism for sublimation fractionation is rate limitation by diffusion of water molecules from the solid-gas interface into the pore spaces between ice grains, analogous to the case for simple evaporative isotope fractionation introduced in Section 1.1. In both models, a thin boundary layer of vapor is in equilibrium with the reservoir. Water molecules diffuse from this boundary layer into the free atmosphere (or pore space) with a characteristic isotopic fractionation. The overall isotopic fractionation depends on the rate of the second step, which varies inversely with relative humidity. Convective air motion within the pore space therefore does not suppress isotopic fractionation and may instead cause greater fractionation if air motions effectively reduce the vapor content inside the firn. This tendency is consistent with the marked isotopic fractionation in snow and ice in the Dry Valleys and Allan Hills BIAs, which are both characterized by windy and low-RH conditions.

The second precondition required for Rayleigh fractionation is isotopic homogenization of the ice reservoir. Specifically, isotopic homogenization of individual ice grains must occur faster than the diffusion of the vapor from the boundary layer into the pore space. Otherwise sublimation becomes "layer-by-layer" and has little isotopic effect. The characteristic timescale for solid-phase diffusion at depth z within an ice grain, $\tau_{diff}(z)$, is:

$$\tau_{diff}(z) = G\frac{r(z)^2}{\kappa_{ice}} \quad (3)$$

where G is a geometrical factor of ~0.057 (Whillans & Grootes, 1985), $r(z)$ is the ice grain radius at depth z, and κ_{ice} is the diffusion coefficient at a given temperature. Equation (3) shows that ice grain size (r) is a primary control on the timescale of solid-state-diffusion, and thus also the

timescale of homogenization. Note that in polar environments, the radius of snow grains increases with depth due to processes resembling Ostwald ripening. Larger grains are often found in warmer sites due to similar reasons. Whether surface snow shows sublimation fractionation thus depends on the relative rates of homogenization and grain growth: beyond a critical grain size, sublimation cannot effectively alter the isotopic composition of snow grains because the grain is too large for diffusion to homogenize it effectively.

Quantitatively, we can evaluate the potential for isotopic homogenization inside ice grains by computing R, the ratio of the residence time (τ_{ice}) of snow layer over depth z (calculated as z over the accumulation rate, A) and the characteristic time of solid-state-diffusion $\tau_{diff}(z)$:

$$R = \frac{\tau_{ice}(z)}{\tau_{diff}(z)} \quad (4)$$

Isotopic fractionation due to sublimation, should it occur, can be propagated into and be recorded in ice grains if $R > 1$. A large value of R indicates that solid-state-diffusion occurs much faster than the rate of grain "advection" to deeper depths, where larger grain sizes might slow homogenization. It should be noted that a greater potential for isotopic homogenization does not mean a larger sublimation mass flux, because sublimation rates depend on other meteorological factors such as relative humidity and wind speed. For $R < 1$, grain-scale isotopic homogenization is slower than grain advection. In this case, sublimation is expected to occur in a "layer-by-layer" fashion without observable isotopic effects.

Now we apply this simple model to different Antarctic sites today to examine whether it can explain why sublimation-induced fractionation is the strongest in the Allan Hills BIA compared to other sites. In Allan Hills, the snow accumulation rate is 0.0075 m yr^{-1}, with a mean

surface grain radius of 0.4 mm that increases with depth at a rate of 0.258 mm m^{-1} until 4.9 m depth, below which no more observations were made (Dadic et al., 2015). Hence, we will limit our discussion to the top 5 m. The present-day mean annual temperature at Allan Hills is -30 °C (Delisle & Sievers, 1991), and the κ_{ice} value at this temperature is 1.5×10^{-8} m^2 yr^{-1} (Waddington et al., 2002). We consider two additional sites for comparison: Dome C, a low accumulation-rate, low-temperature site, and Siple Dome, a high-accumulation, temperate site. At Dome C, the grain radius is 0.1 mm at the surface and increases to 0.3 mm at 1 m depth, below which it remains somewhat constant (Gay et al., 2002). No grain-radius data are available below 3 m, so we assume here that it remains constant to 5 m depth. At Siple Dome, the grain radius at the surface is ~0.2 mm and increases to ~0.7 mm at 5 m depth (Alley & Bentley, 1988). With a mean annual temperature of -55 °C at Dome C (Petit et al., 1982) and -26.5 °C at Siple Dome (Alley & Bentley, 1988), the κ_{ice} values are calculated to be 4.8×10^{-10} m^2 yr^{-1} and 2.3×10^{-8} m^2 yr^{-1} at Dome C and Siple Dome, respectively.

Using these input variables, we calculate R as a function of depth at each site (Figure 6). A few observations can be made. First, below 1 m depth, the rate of solid-phase-diffusion is much faster than the grain advection, consistent with earlier findings by (Waddington et al., 2002) that identified other processes such as the vertical motion of interstitial vapor by diffusion to be suppressing the expression of isotopic signals. Second, within a few centimeters at the top, where sublimation has been observed to be most pronounced (Hughes et al., 2021), the rate of solid-phase-diffusion is slower than the grain advection. In warm sites with high accumulation rates such as Siple Dome, R is persistently greater than 1 to allow grain-scale homogenization. However, because Siple Dome is situated within 500 km of the West Antarctic coastline, input of moist air suppresses sublimation of the surface snow. On the other hand, in cold, low-

accumulation-rate sites such as Dome C, while the low-RH conditions are conducive to snow mass loss by sublimation, R remains low (< 1) at the top 4 cm of the snow because of the low temperatures; isotopic homogenization of the grains is disfavored. As a result, sublimation does not usually change the isotopic composition of snow in typical ice core sites unless two seemingly contradictory conditions are present: a dry, windy environment that promotes sublimation and a relatively warm mean annual temperature that allows fast isotopic homogenization within snow grains via solid-state-diffusion. Such conditions can be found in sites such as Allan Hills and Dry Valleys today, which explains why negative d-excess values are only observed there.

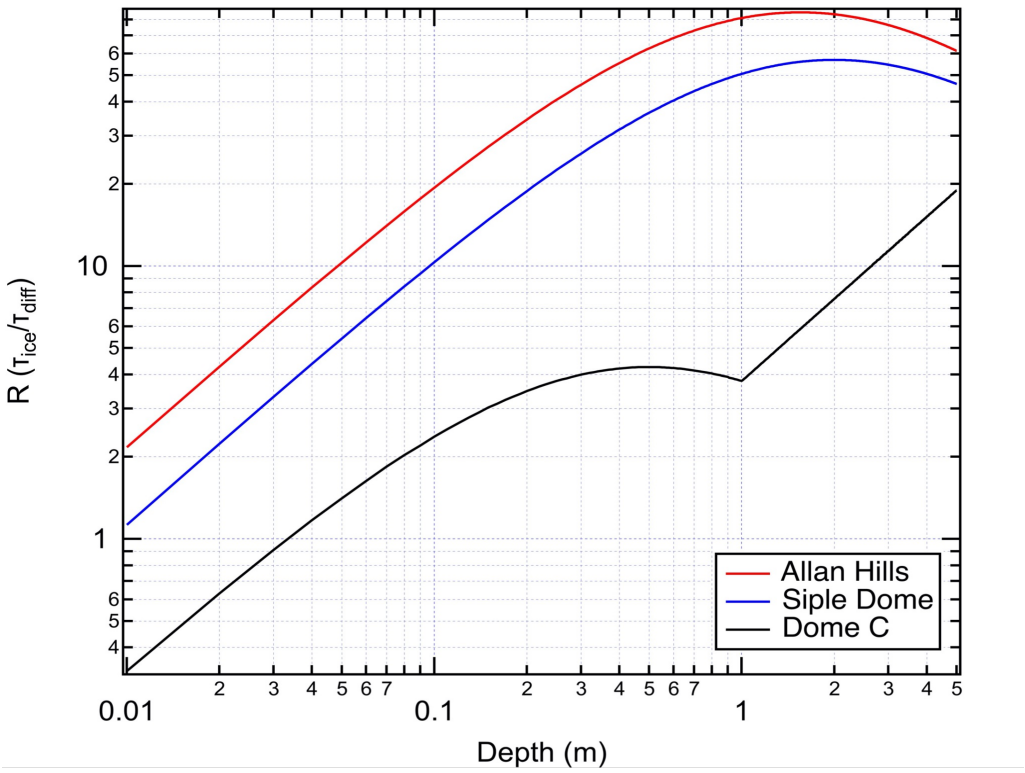

Figure 6. Ratios of τ_{ice}/τ_{diff} under different polar conditions. Dome C represents cold, low accumulation rate regimes, while Siple Dome represents warm, high accumulation rate regimes.

4.2 *Quantifying potential effects of sublimation on the isotopic composition of surface snow*

Now we calculate if sublimation is the only process that changes snow d-excess values, how much ice must be lost in order to yield the negative d-excess observed in the Allan Hills surface snow [-5‰; (Dadic et al., 2015)]. We note that this negative value is also observed in blue ice dating back to the interglacial periods (based on ice δD) around ~300 ka (Higgins et al., 2015). Having shown that solid-state-diffusion can transmit the isotopic signal at the grain-vapor boundary into the whole ice grains, we will describe isotopic fractionation of freshly deposited firn using a Rayleigh distillation model. We assume that a thin layer of sublimed vapor is in equilibrium with the firn and the vapor [the equilibrium fractionation factor for sublimation calculated from (Ellehoj et al., 2013)], and can be kinetically fractionated as it diffuses into the pore space as well as into the free atmosphere.

We considered two end-member scenarios: (1) RH of 0, where effective molecular diffusion fractionation factors [0.9757 for HDO/H_2O and 0.9727 for $H_2{}^{18}O/H_2{}^{16}O$ (Merlivat, 1978)] dictate the kinetic fractionation factors and (2) RH of 1, when the kinetic fractionation vanishes. The actual sublimation regime in the Dry Valleys region is not clear, but should reside somewhere between these two end-members. For this calculation, a site temperature of -30°C was used (Delisle & Sievers, 1991). The initial δD, $\delta^{18}O$, and d-excess values used in our Rayleigh model are -270‰, -34‰, and 2‰, respectively, which are observed values in modern Allan Hills snow at 30-cm depth reported by (Dadic et al., 2015). Note that we did not use the isotopic values of the surface snow observed in (Dadic et al., 2015), which has a negative d-excess value, suggesting the snow may have been subject to sublimation. As a matter of fact, we

563 do not know the true initial composition of the freshly deposited snow, and no measurements of
564 the d-excess of precipitation in the Allan Hills region are available.

565 The Rayleigh model predicts that 3% (RH = 0) to 24% (RH = 1) of the snow must be lost
566 to sublimation in order to yield the -5‰ d-excess observed in the Allan Hills surface snow and
567 blue ice samples (Figure 7a). Rayleigh fractionation would also elevate $\delta^{18}O$ values of the
568 remaining ice grains by between 1.4‰ (RH = 0) and 5.6‰ (RH =1) (Figure 7b).

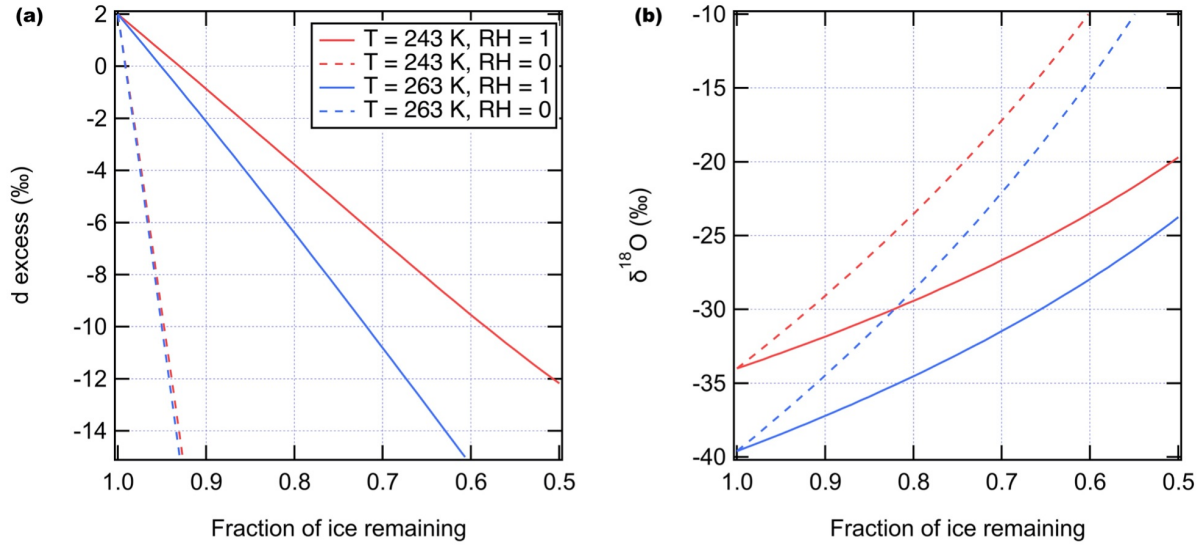

569

570 **Figure 7.** Quantifying the effect of sublimation on d-excess (a) and $\delta^{18}O$ (b) in the remaining
571 snow using a Rayleigh-distillation model under interglacial (red) and glacial (blue) conditions.

572

573 *4.3 Implications for paleotemperature reconstructions*

574 Now we return to an earlier question why the $\delta^{18}O$-temperature relationship observed in
575 ice cores can at times be different from the present-day spatial $\delta^{18}O$-temperature relationship.
576 There must exist processes that differentially alter the characteristic relationship at different
577 temperatures. For example, moisture sources (Vimeux et al., 1999) and ice sheet topography

(Buizert et al., 2021; Werner et al., 2018) have been proposed to explain the variations in the temporal $\delta^{18}O$-temperature relationship. The results presented in this study provide an additional mechanism that can alter the isotope-temperature slopes: a varying fraction of snow lost to sublimation.

To investigate the sublimation effect in the case of glacial Allan Hills ice, we built upon the Rayleigh distillation framework described above to quantify the potential effects of sublimation-induced fractionation on the temporal isotope-temperature slope. The surface temperature is assumed to be 7 °C cooler than interglacial, equivalent to the glacial-interglacial temperature difference observed in the nearby (~500 km) Talos Dome ice core (Buizert et al., 2021). We also assumed that the modern spatial slope applies in temperature conversion to "primary" isotopic changes, before the effects of sublimation are considered. This glacial cooling lowers the precipitation $\delta^{18}O$ and δD by 5.6‰ and 44.8‰, respectively. An implicit assumption behind this calculation is that precipitation d-excess remains the same. We acknowledge that this assumption may be over-simplified, because d-excess values in glacial times are indeed ~4‰ lower than interglacial d-excess values in both inland and coastal ice core sites in East Antarctica (Stenni et al., 2010; Vimeux, Masson, Delaygue, et al., 2001). The point here is to demonstrate the capability of sublimation in modifying the observed isotope-temperature relationship, and should be treated as an upper limit of the impact of sublimation on glacial snow. Quantitatively constraining the magnitude of surface snow sublimation during glacial times requires iCESM simulations to be run under glacial conditions, which is beyond the scope of this study.

On the basis of these simplified glacial boundary conditions, we calculated the effect of sublimation on the isotopic composition of snow in glacial Allan Hills. To yield a d-excess of -10‰ [the lower limit of d-excess observed in Allan Hills ice cores (Figure 5) (Higgins et al.,

2015)], between 5% (RH = 0) and 28% (RH = 1) of the ice would need to be lost by sublimation (Figure 7a). $\delta^{18}O$ values of ice would then increase by 2.5‰ (RH = 0) to 7.5‰ (RH = 1) relative to the precipitation that initially fell (Figure 7b). By comparison, the modern-day (interglacial) increase in $\delta^{18}O$ value due to sublimation was calculated in Section 4.2 to be between 1.4‰ (RH = 0) and 5.6‰ (RH =1). In both RH scenarios, the greater sublimation-induced enrichment of $\delta^{18}O$ during glacial periods leads to a temporal $\delta^{18}O$ slope of 0.5 (RH = 1) to 0.6 (RH = 0) ‰/°C, close to the independently constrained temporal slope of 0.5‰/°C obtained by (Steig et al., 2000). We note that the effect of sublimation and other factors such as varying moisture source conditions and ice-sheet topography changes are not mutually exclusive. However, it is clear that in low-accumulation-rate regimes, sublimation alone can significantly alter the isotope-temperature relationship.

A number of factors could influence the fraction of ice being lost due to sublimation during the glacial intervals. First, accumulation rates are lower in glacial than in interglacial periods by a factor of 2 to 3 (Siegert, 2003). The residence time of snow in the surface sublimation zone would be lengthened accordingly, increasing the sublimation potential (*R* values calculated in Section 4.1). In addition, polar regions in glacial intervals are generally characterized by windier and drier conditions, promoting the forced ventilation of vapor inside the firn. However, lower surface temperature inhibits solid-phase-diffusion as well as vapor diffusion into the pore space. Overall, it appears that accumulation rates play a more important role in Allan Hills, and more firn ice is lost due to sublimation during glacial periods than in interglacials. An apparent glacial warming due to the stronger enrichment effect in the ice core $\delta^{18}O$ and δD records would ensue.

To summarize, the sublimation of freshly deposited snow could be enhanced in glacial periods, leading to larger glacial firn-ice $\delta^{18}O$ and δD increases than in interglacial periods and thus a shallower temporal isotope-temperature slope during these intervals. Our results reinforce the necessity of independent temperature constraints such as borehole temperatures. In the case of Allan Hills, where no such independent temperature estimates are available, applying the conventional 0.8‰/°C spatial slope to isotope records obtained from those sites would likely lead to an underestimate of the magnitude of glacial (and longer-term) cooling.

4.4 Implications for isotope-enabled climate models

While the land component of iCESM considers sublimation of surface snow and ice, sublimation is assumed to be a non-fractionating process (Dütsch et al., 2019). However, we show that in a low accumulation site (0.0075 m yr^{-1}) today, 3-24% of snow at the surface could be lost due to sublimation, accompanied by a lowering of the surface snow d-excess value of 7‰ (from 2‰ to -5‰). During glacial periods, the fraction of the snow lost due to sublimation could be as high as 28%. Sublimation also elevates the δD and $\delta^{18}O$ values of the remaining ice. At the same time, the sublimed vapor has lower δD and $\delta^{18}O$ values and higher d-excess values compared to the remaining snow, constituting a potentially important secondary source of vapor in Antarctica (Kopec et al., 2019; Pang et al., 2019). Overall, our modeling results underscore the necessity of including fractionation during sublimation into surface mass and isotope balance in Antarctica in future versions of the iCESM land model. We note that certain forward models for high-elevation mountain ice cores have attempted to parameterize sublimation and take isotopic fractionation into account (Hurley et al., 2016). However, we acknowledge that any parameters, such as factors that determine the sublimation rate, are still under-constrained *in situ*.

5. Conclusions

Using an isotope-enable climate model, we showed that the negative d-excess observed in ice cores and surface ice samples from Allan Hills and the Dry Valleys cannot be realistically reproduced by current-generation climate models, indicating post-depositional alterations due to sublimation. Sublimation likely altered the isotopic composition of the snow, lowering d-excess and enriching δD and $\delta^{18}O$. This is in contrast to the earlier assumption that sublimation occurs layer-by-layer with no isotopic fractionation. We identified that the long residence time of snow on the surface could allow for isotopic homogenization of individual ice grains by solid-phase-diffusion, a key physical mechanism that alters the isotopic composition (including d-excess) of snow. However, if the temperature is too low, solid-phase-diffusion will be inhibited and no fractionation is observed. Our simple model explains why most ice core isotope records are not appreciably impacted by sublimation, because site conditions either are not conducive to sublimation (warm and calm) or do not allow isotopic homogenization (cold). Nevertheless, when dry, windy, and relatively warm conditions like those characterizing the Dry Valleys and Allan Hills do allow isotopic fractionation by sublimation, this process should be taken into account in order to accurately interpret past temperature from ice δD and $\delta^{18}O$. Future isotope-enabled climate models should also explicitly simulate sublimation to improve our understanding of the connections between climate conditions and the isotope record preserved in ice cores.

Acknowledgments

This work is supported by the Pan Postdoctoral Research Fellowship, The David and Lucile Packard Foundation, and the Department of Earth, Environmental, and Planetary Sciences at Rice University. The simulation data used in this study are available online (https://doi.org/10.5281/zenodo.5523287).

669 **References**

670 Alley, R. B., & Bentley, C. R. (1988). Ice-Core Analysis on the Siple Coast of West Antarctica.
671 *Annals of Glaciology*, *11*, 1–7. https://doi.org/10.1017/s0260305500006236

672 Bailey, A., Singh, H. K. A., & Nusbaumer, J. (2019). Evaluating a moist isentropic framework
673 for poleward moisture transport: implications for water isotopes over Antarctica.
674 *Geophysical Research Letters*, *46*, 7819–7827. https://doi.org/10.1029/2019GL082965

675 Benetti, M., Reverdin, G., Pierre, C., Merlivat, L., Risi, C., Steen-Larsen, H. C., & Vimeux, F.
676 (2014). Deuterium excess in marine water vapor: Dependency on relative humidity and
677 surface wind speed during evaporation. *Journal of Geophysical Research: Atmospheres*,
678 *119*(2), 584–593. https://doi.org/10.1002/2013jd020535

679 Bintanja, R. (1999). On the glaciological, meteorological, and climatological significance of
680 Antarctic blue ice areas. *Reviews of Geophysics*, *37*(3), 337–359.
681 https://doi.org/10.1029/1999rg900007

682 Bliss, A. K., Cuffey, K. M., & Kavanaugh, J. L. (2011). Sublimation and surface energy budget
683 of Taylor Glacier, Antarctica. *Journal of Glaciology*, *57*(204), 684–696.
684 https://doi.org/10.3189/002214311797409767

685 Brady, E., Stevenson, S., Bailey, D., Liu, Z., Noone, D., Nusbaumer, J., et al. (2019). The
686 connected isotopic water cycle in the Community Earth System Model version 1. *Journal of*
687 *Advances in Modeling Earth Systems*, *11*(8), 2547–2566.
688 https://doi.org/10.1029/2019ms001663

689 Buizert, C., Gkinis, V., Severinghaus, J. P., He, F., Lecavalier, B. S., Kindler, P., et al. (2014).
690 Greenland temperature response to climate forcing during the last deglaciation. *Science*,

345(6201), 1177–1180. https://doi.org/10.1126/science.1254961

Buizert, C., Fudge, T. J., Roberts, W. H. G., Steig, E. J., Sherriff-Tadano, S., Ritz, C., et al. (2021). Antarctic surface temperature and elevation during the Last Glacial Maximum. *Science*, *372*(6546), 1097–1101. https://doi.org/10.1126/science.abd2897

Casado, M., Landais, A., Masson-Delmotte, V., Genthon, C., Kerstel, E., Kassi, S., et al. (2016). Continuous measurements of isotopic composition of water vapour on the East Antarctic Plateau. *Atmospheric Chemistry and Physics*, *16*(13), 8521–8538. https://doi.org/10.5194/acp-16-8521-2016

Casado, M., Landais, A., Picard, G., Münch, T., Laepple, T., Stenni, B., et al. (2018). Archival processes of the water stable isotope signal in East Antarctic ice cores. *The Cryosphere*, *12*(5), 1745–1766. https://doi.org/10.5194/tc-12-1745-2018

Ciais, P., & Jouzel, J. (1994). Deuterium and oxygen 18 in precipitation: Isotopic model, including mixed cloud processes. *Journal of Geophysical Research*, *99*(D8), 16793. https://doi.org/10.1029/94jd00412

Craig, H., & Gordon, L. I. (1965). Deuterium and Oxygen 18 Variations in the Ocean and the Marine Atmosphere. In E. Tongiorgi (Ed.), *Stable Isotopes in Oceanographic Studies and Paleotemperatures* (pp. 9–130). Spoleto: Conferences in Nuclear Geology.

Cuffey, K. M., & Clow, G. D. (1997). Temperature, accumulation, and ice sheet elevation in central Greenland through the last deglacial transition. *Journal of Geophysical Research: Oceans*, *102*(C12), 26383–26396. https://doi.org/10.1029/96jc03981

Cuffey, K. M., & Steig, E. J. (1998). Isotopic diffusion in polar firn: implications for interpretation of seasonal climate parameters in ice-core records, with emphasis on central

713 Greenland. *Journal of Glaciology*, *44*(147), 273–284.
714 https://doi.org/10.1017/s0022143000002616

715 Cuffey, K. M., Clow, G. D., Steig, E. J., Buizert, C., Fudge, T. J., Koutnik, M., et al. (2016).
716 Deglacial temperature history of West Antarctica. *Proceedings of the National Academy of*
717 *Sciences of the United States of America*, *113*(50), 14249–14254.
718 https://doi.org/10.1073/pnas.1609132113

719 Dadic, R., Schneebeli, M., Bertler, N. A. N., Schwikowski, M., & Matzl, M. (2015). Extreme
720 snow metamorphism in the Allan Hills, Antarctica, as an analogue for glacial conditions
721 with implications for stable isotope composition. *Journal of Glaciology*, *61*(230), 1171–
722 1182. https://doi.org/10.3189/2015jog15j027

723 Dansgaard, W. (1964). Stable isotopes in precipitation. *Tellus*, *16*(4), 436–468.
724 https://doi.org/10.1111/j.2153-3490.1964.tb00181.x

725 Delisle, G., & Sievers, J. (1991). Sub-ice topography and meteorite finds near the Allan Hills and
726 the Near Western Ice Field, Victoria Land, Antarctica. *Journal of Geophysical Research:*
727 *Planets*, *96*(E1), 15577–15587. https://doi.org/10.1029/91je01117

728 Dütsch, M., Blossey, P. N., Steig, E. J., & Nusbaumer, J. M. (2019). Nonequilibrium
729 Fractionation During Ice Cloud Formation in iCAM5: Evaluating the Common
730 Parameterization of Supersaturation as a Linear Function of Temperature. *Journal of*
731 *Advances in Modeling Earth Systems*, *11*(11), 3777–3793.
732 https://doi.org/10.1029/2019ms001764

733 Dyer, E. L. E., Jones, D. B. A., Nusbaumer, J., Li, H., Collins, O., Vettoretti, G., & Noone, D.
734 (2017). Congo Basin precipitation: Assessing seasonality, regional interactions, and sources

735 of moisture. *Journal of Geophysical Research*, *122*(13), 6882–6898.
736 https://doi.org/10.1002/2016jd026240

737 Ellehoj, M. D., Steen-Larsen, H. C., Johnsen, S. J., & Madsen, M. B. (2013). Ice-vapor
738 equilibrium fractionation factor of hydrogen and oxygen isotopes: experimental
739 investigations and implications for stable water isotope studies. *Rapid Communications in*
740 *Mass Spectrometry: RCM*, *27*(19), 2149–2158. https://doi.org/10.1002/rcm.6668

741 Friedman, I., Benson, C., & Gleason, J. (1991). Isotopic changes during snow metamorphism. In
742 *Stable isotope geochemistry: a tribute to Samuel Epstein* (pp. 211–221).

743 Gat, J. R., Klein, B., Kushnir, Y., Roether, W., Wernli, H., Yam, R., & Shemesh, A. (2011).
744 Isotope composition of air moisture over the Mediterranean Sea: an index of the air-sea
745 interaction pattern. *Tellus B: Chemical and Physical Meteorology*, *55*(5), 953–965.
746 https://doi.org/10.3402/tellusb.v55i5.16395

747 Gay, M., Fily, M., Genthon, C., Frezzotti, M., Oerter, H., & Winther, J.-G. (2002). Snow grain-
748 size measurements in Antarctica. *Journal of Glaciology*, *48*(163), 527–535.
749 https://doi.org/10.3189/172756502781831016

750 Gooseff, M. N., Berry Lyons, W., McKnight, D. M., Vaughn, B. H., Fountain, A. G., &
751 Dowling, C. (2006). A Stable Isotopic Investigation of a Polar Desert Hydrologic System,
752 McMurdo Dry Valleys, Antarctica. *Arctic, Antarctic, and Alpine Research*, *38*(1), 60–71.
753 https://doi.org/10.1657/1523-0430(2006)038[0060:asiioa]2.0.co;2

754 Grootes, P. M., Stuiver, M., White, J. W. C., Johnsen, S., & Jouzel, J. (1993). Comparison of
755 oxygen isotope records from the GISP2 and GRIP Greenland ice cores. *Nature*, *366*(6455),
756 552–554. https://doi.org/10.1038/366552a0

Higgins, J. A., Kurbatov, A. V., Spaulding, N. E., Brook, E., Introne, D. S., Chimiak, L. M., et al. (2015). Atmospheric composition 1 million years ago from blue ice in the Allan Hills, Antarctica. *Proceedings of the National Academy of Sciences of the United States of America*, *112*(22), 6887–6891. https://doi.org/10.1073/pnas.1420232112

Holloway, M. D., Sime, L. C., Singarayer, J. S., Tindall, J. C., & Valdes, P. J. (2018). Simulating the 128-ka Antarctic Climate Response to Northern Hemisphere Ice Sheet Melting Using the Isotope-Enabled HadCM3. *Geophysical Research Letters*, *45*(21), 11,921–11,929. https://doi.org/10.1029/2018gl079647

Hughes, A. G., Jones, T. R., Vinther, B. M., Gkinis, V., Max Stevens, C., Morris, V., et al. (2020). High-frequency climate variability in the Holocene from a coastal-dome ice core in east-central Greenland. *Climate of the Past*, *16*(4), 1369–1386. https://doi.org/10.5194/cp-16-1369-2020

Hughes, A. G., Wahl, S., Jones, T. R., Zuhr, A., Hörhold, M., White, J. W. C., & Steen-Larsen, H. C. (2021, April 14). *The role of sublimation as a driver of climate signals in the water isotope content of surface snow: Laboratory and field experimental results*. *The Cryosphere*. https://doi.org/10.5194/tc-2021-87

Hu, J., Emile-Geay, J., Tabor, C., Nusbaumer, J., & Partin, J. (2019). Deciphering Oxygen Isotope Records From Chinese Speleothems With an Isotope-Enabled Climate Model. *Paleoceanography and Paleoclimatology*, *34*(12), 2098–2112. https://doi.org/10.1029/2019pa003741

Hurley, J. V., Vuille, M., & Hardy, D. R. (2016). Forward modeling of $\delta^{18}O$ in Andean ice cores. *Geophysical Research Letters*, *43*(15), 8178–8188. https://doi.org/10.1002/2016gl070150

779 Jones, T. R., Cuffey, K. M., White, J. W. C., Steig, E. J., Buizert, C., Markle, B. R., et al. (2017).
780 Water isotope diffusion in the WAIS Divide ice core during the Holocene and last glacial.
781 *Journal of Geophysical Research: Earth Surface*, *122*(1), 290–309.
782 https://doi.org/10.1002/2016jf003938

783 Jones, T. R., Roberts, W. H. G., Steig, E. J., Cuffey, K. M., Markle, B. R., & White, J. W. C.
784 (2018). Southern Hemisphere climate variability forced by Northern Hemisphere ice-sheet
785 topography. *Nature*, *554*(7692), 351–355. https://doi.org/10.1038/nature24669

786 Jouzel, J., & Merlivat, L. (1984). Deuterium and oxygen 18 in precipitation: Modeling of the
787 isotopic effects during snow formation. *Journal of Geophysical Research*, *89*(D7), 11749.
788 https://doi.org/10.1029/jd089id07p11749

789 Jouzel, J., Merlivat, L., & Lorius, C. (1982). Deuterium excess in an East Antarctic ice core
790 suggests higher relative humidity at the oceanic surface during the last glacial maximum.
791 *Nature*, *299*(5885), 688–691. https://doi.org/10.1038/299688a0

792 Jouzel, J., Masson-Delmotte, V., Cattani, O., Dreyfus, G., Falourd, S., Hoffmann, G., et al.
793 (2007). Orbital and millennial Antarctic climate variability over the past 800,000 years.
794 *Science*, *317*(5839), 793–796. https://doi.org/10.1126/science.1141038

795 Kalnay, E., Kanamitsu, M., Kistler, R., Collins, W., Deaven, D., Gandin, L., et al. (1996). The
796 NCEP/NCAR 40-year reanalysis project. *B. Am. Meteorol. Soc.*, *77*, 437–471.

797 Kopec, B. G., Feng, X., Posmentier, E. S., & Sonder, L. J. (2019). Seasonal Deuterium Excess
798 Variations of Precipitation at Summit, Greenland, and their Climatological Significance.
799 *Journal of Geophysical Research: Atmospheres*, *124*(1), 72–91.
800 https://doi.org/10.1029/2018jd028750

Li, C., Ren, J., Shi, G., Pang, H., Wang, Y., Hou, S., et al. (2021). Spatial and temporal variations of fractionation of stable isotopes in East-Antarctic snow. *Journal of Glaciology*, *67*(263), 523–532. https://doi.org/10.1017/jog.2021.5

Lorius, C., Merlivat, L., & Hagemann, R. (1969). Variation in the mean deuterium content of precipitations in Antarctica. *Journal of Geophysical Research*, *74*(28), 7027–7031. https://doi.org/10.1029/jc074i028p07027

Madsen, M. V., Steen-Larsen, H. C., Hörhold, M., Box, J., Berben, S. M. P., Capron, E., et al. (2019). Evidence of Isotopic Fractionation During Vapor Exchange Between the Atmosphere and the Snow Surface in Greenland. *Journal of Geophysical Research, D: Atmospheres*, *124*(6), 2932–2945. https://doi.org/10.1029/2018JD029619

Masson-Delmotte, V., Hou, S., Ekaykin, A., Jouzel, J., Aristarain, A., Bernardo, R. T., et al. (2008). A review of Antarctic surface snow isotopic composition: Observations, atmospheric circulation, and isotopic modeling. *Journal of Climate*, *21*(13), 3359–3387. https://doi.org/10.1175/2007jcli2139.1

Merlivat, L. (1978). Molecular diffusivities of $H_2{}^{16}O$, $HD^{16}O$, and $H_2{}^{18}O$ in gases. *The Journal of Chemical Physics*, *69*(6), 2864. https://doi.org/10.1063/1.436884

Mezgec, K., Stenni, B., Crosta, X., Masson-Delmotte, V., Baroni, C., Braida, M., et al. (2017). Holocene sea ice variability driven by wind and polynya efficiency in the Ross Sea. *Nature Communications*, *8*(1), 1334. https://doi.org/10.1038/s41467-017-01455-x

Moser, H., & Stichler, W. (1974). Deutenum and oxygen-18 contents as an index of the properties of snowblankets. In *Int. Symp. Snow Mechanics (IUGG, IASH, ICSI)*. Grindelwald, Switzerland.

Nusbaumer, J., & Noone, D. (2018). Numerical Evaluation of the Modern and Future Origins of Atmospheric River Moisture over the West Coast of the United States. *Journal of Geophysical Research, D: Atmospheres*, *123*(12), 6423–6442. https://doi.org/10.1029/2017JD028081

Nusbaumer, J., Wong, T. E., Bardeen, C., & Noone, D. (2017). Evaluating hydrological processes in the Community Atmosphere Model Version 5 (CAM5) using stable isotope ratios of water. *Journal of Advances in Modeling Earth Systems*, *9*(2), 949–977. https://doi.org/10.1002/2016MS000839

Pang, H., Hou, S., Landais, A., Masson-Delmotte, V., Jouzel, J., Steen-Larsen, H. C., et al. (2019). Influence of Summer Sublimation on δD, $\delta^{18}O$, and $\delta^{17}O$ in Precipitation, East Antarctica, and Implications for Climate Reconstruction From Ice Cores. *Journal of Geophysical Research: Atmospheres*, *124*, 7339–7358. https://doi.org/10.1029/2018jd030218

Petit, J. R., Jouzel, J., Pourchet, M., & Merlivat, L. (1982). A detailed study of snow accumulation and stable isotope content in Dome C (Antarctica). *Journal of Geophysical Research*, *87*(C6), 4301. https://doi.org/10.1029/jc087ic06p04301

Petit, J. R., White, J. W. C., Young, N. W., Jouzel, J., & Korotkevich, Y. S. (1991). Deuterium excess in recent Antarctic snow. *Journal of Geophysical Research*, *96*(D3), 5113. https://doi.org/10.1029/90jd02232

Petit, J. R., Jouzel, J., Raynaud, D., Barkov, N. I., Barnola, J.-M., Basile, I., et al. (1999). Climate and atmospheric history of the past 420,000 years from the Vostok ice core, Antarctica. *Nature*, *399*(6735), 429–436. https://doi.org/10.1038/20859

Pfahl, S., & Sodemann, H. (2014). What controls deuterium excess in global precipitation? *Climate of the Past*, *10*, 771–781. https://doi.org/10.5194/cp-10-771-2014

Rayner, N. A., Parker, D. E., Horton, E. B., Folland, C. K., Alexander, L. V., Rowell, D. P., et al. (2003). Global analyses of sea surface temperature, sea ice, and night marine air temperature since the late nineteenth century. *Journal of Geophysical Research*, *108*(D14). https://doi.org/10.1029/2002jd002670

Ritter, F., Steen-Larsen, H. C., Werner, M., Masson-Delmotte, V., Orsi, A., Behrens, M., et al. (2016). Isotopic exchange on the diurnal scale between near-surface snow and lower atmospheric water vapor at Kohnen station, East Antarctica. *The Cryosphere*, *10*(4), 1647–1663. https://doi.org/10.5194/tc-10-1647-2016

Severinghaus, J. P., Albert, M. R., Courville, Z. R., Fahnestock, M. A., Kawamura, K., Montzka, S. A., et al. (2010). Deep air convection in the firn at a zero-accumulation site, central Antarctica. *Earth and Planetary Science Letters*, *293*(3-4), 359–367. https://doi.org/10.1016/j.epsl.2010.03.003

Siegert, M. J. (2003). Glacial–interglacial variations in central East Antarctic ice accumulation rates. *Quaternary Science Reviews*, *22*(5-7), 741–750. https://doi.org/10.1016/s0277-3791(02)00191-9

Singh, H. K. A., Donohoe, A., Bitz, C. M., Nusbaumer, J., & Noone, D. C. (2016). Greater aerial moisture transport distances with warming amplify interbasin salinity contrasts. *Geophysical Research Letters*, *43*(16), 8677–8684. https://doi.org/10.1002/2016gl069796

Sodemann, H., & Stohl, A. (2009). Asymmetries in the moisture origin of Antarctic precipitation. *Geophysical Research Letters*, *36*, L22803.

https://doi.org/10.1029/2009gl040242

Sokratov, S. A., & Golubev, V. N. (2009). Snow isotopic content change by sublimation. *Journal of Glaciology*, *55*(193), 823–828. https://doi.org/10.3189/002214309790152456

Spaulding, N. E., Spikes, V. B., Hamilton, G. S., Mayewski, P. A., Dunbar, N. W., Harvey, R. P., et al. (2012). Ice motion and mass balance at the Allan Hills blue-ice area, Antarctica, with implications for paleoclimate reconstructions. *Journal of Glaciology*, *58*(208), 399–406. https://doi.org/10.3189/2012jog11j176

Steen-Larsen, H. C., Masson-Delmotte, V., Hirabayashi, M., Winkler, R., Satow, K., Prié, F., et al. (2014). What controls the isotopic composition of Greenland surface snow? *Climate of the Past*, *10*(1), 377–392. https://doi.org/10.5194/cp-10-377-2014

Steig, E. J., Morse, D. L., Waddington, E. D., Stuiver, M., Grootes, P. M., Mayewski, P. A., et al. (2000). Wisconsinan and holocene climate history from an ice core at taylor dome, western ross embayment, antarctica. *Geografiska Annaler: Series A, Physical Geography*, *82*(2-3), 213–235. https://doi.org/10.1111/j.0435-3676.2000.00122.x

Steig, E. J., Jones, T. R., Schauer, A. J., Kahle, E. C., Morris, V. A., Vaughn, B. H., et al. (2021). Continuous-Flow Analysis of δ17O, δ18O, and δD of H2O on an Ice Core from the South Pole. *Frontiers in Earth Science*, *9*, 640292. https://doi.org/10.3389/feart.2021.640292

Stenni, B., Masson-Delmotte, V., Selmo, E., Oerter, H., Meyer, H., Röthlisberger, R., et al. (2010). The deuterium excess records of EPICA Dome C and Dronning Maud Land ice cores (East Antarctica). *Quaternary Science Reviews*, *29*(1-2), 146–159. https://doi.org/10.1016/j.quascirev.2009.10.009

Stichler, W., Schotterer, U., Fröhlich, K., Ginot, P., Kull, C., Gäggeler, H., & Pouyaud, B.

(2001). Influence of sublimation on stable isotope records recovered from high-altitude glaciers in the tropical Andes. *Journal of Geophysical Research: Atmospheres*, *106*(D19), 22613–22620. https://doi.org/10.1029/2001jd900179

Tabor, C. R., Otto-Bliesner, B. L., Brady, E. C., Nusbaumer, J., Zhu, J., Erb, M. P., et al. (2018). Interpreting Precession-Driven δ18O Variability in the South Asian Monsoon Region. *Journal of Geophysical Research: Atmospheres*, *123*, 5927– 5946. https://doi.org/10.1029/2018JD028424

Uemura, R., Matsui, Y., Yoshimura, K., Motoyama, H., & Yoshida, N. (2008). Evidence of deuterium excess in water vapor as an indicator of ocean surface conditions. *Journal of Geophysical Research*, *113*(D19). https://doi.org/10.1029/2008jd010209

Uemura, R., Masson-Delmotte, V., Jouzel, J., Landais, A., Motoyama, H., & Stenni, B. (2012). Ranges of moisture-source temperature estimated from Antarctic ice cores stable isotope records over glacial–interglacial cycles. *Climate of the Past*, *8*(3), 1109–1125. https://doi.org/10.5194/cp-8-1109-2012

Vimeux, F., Masson, V., Jouzel, J., Stievenard, M., & Petit, J. R. (1999). Glacial–interglacial changes in ocean surface conditions in the Southern Hemisphere. *Nature*, *398*(6726), 410–413. https://doi.org/10.1038/18860

Vimeux, F., Masson, V., Delaygue, G., Jouzel, J., Petit, J. R., & Stievenard, M. (2001). A 420,000 year deuterium excess record from East Antarctica: Information on past changes in the origin of precipitation at Vostok. *Journal of Geophysical Research: Atmospheres*, *106*(D23), 31863–31873. https://doi.org/10.1029/2001jd900076

Vimeux, F., Masson, V., Jouzel, J., Petit, J. R., Steig, E. J., Stievenard, M., et al. (2001).

911 Holocene hydrological cycle changes in the Southern Hemisphere documented in East
912 Antarctic deuterium excess records. *Climate Dynamics*, *17*(7), 503–513.
913 https://doi.org/10.1007/pl00007928

914 Waddington, E. D., Steig, E. J., & Neumann, T. A. (2002). Using characteristic times to assess
915 whether stable isotopes in polar snow can be reversibly deposited. *Annals of Glaciology*, *35*,
916 118–124. https://doi.org/10.3189/172756402781817004

917 Wang, H., Fyke, J. G., Lenaerts, J., Nusbaumer, J. M., Singh, H., Noone, D., et al. (2020).
918 Influence of sea-ice anomalies on Antarctic precipitation using source attribution in the
919 Community Earth System Model. *The Cryosphere*, *14*(2), 429–444.
920 https://doi.org/10.5194/tc-14-429-2020

921 Werner, M., Jouzel, J., Masson-Delmotte, V., & Lohmann, G. (2018). Reconciling glacial
922 Antarctic water stable isotopes with ice sheet topography and the isotopic
923 paleothermometer. *Nature Communications*, *9*(1), 3537. https://doi.org/10.1038/s41467-
924 018-05430-y

925 Whillans, I. M., & Grootes, P. M. (1985). Isotopic diffusion in cold snow and firn. *Journal of*
926 *Geophysical Research*, *90*(D2), 3910. https://doi.org/10.1029/jd090id02p03910

927 Yan, Y., Bender, M. L., Brook, E. J., Clifford, H. M., Kemeny, P. C., Kurbatov, A. V., et al.
928 (2019). Two-million-year-old snapshots of atmospheric gases from Antarctic ice. *Nature*,
929 *574*(7780), 663–666. https://doi.org/10.1038/s41586-019-1692-3

930 Yau, M. K., & Rogers, R. R. (1996). *A Short Course in Cloud Physics*. Saint Louis, MO:
931 Elsevier Science.

932